PHYSICAL REVIEW B **80**, 075431 (2009)

Angle-resolved photoemission study of the graphite intercalation compound KC_8: A key to graphene

A. Grüneis,[1,2,*] C. Attaccalite,[3] A. Rubio,[3,4] D. V. Vyalikh,[5] S. L. Molodtsov,[5] J. Fink,[2,6] R. Follath,[6] W. Eberhardt,[6] B. Büchner,[2] and T. Pichler[1]

[1]*Faculty of Physics, Vienna University, Strudlhofgasse 4, 1090 Wien, Austria*

[2]*IFW Dresden, P.O. Box 270116, D-01171 Dresden, Germany*

[3]*Nano-Bio Spectroscopy Group and ETSF Scientific Development Centre, Dpto. Física de Materiales, Universidad del País Vasco, Centro de Física de Materiales CSIC-UPV/EHU-MPC and DIPC, Av. Tolosa 72, E-20018 San Sebastián, Spain*

[4]*Fritz-Haber-Institute of the Max Planck Society, Theory Department, Faradayweg 4-6, D-14195 Berlin-Dahlem, Germany*

[5]*Institut für Festkörperphysik, TU Dresden, Mommsenstrasse 13, D-01069 Dresden, Germany*

[6]*Helmholtz-Zentrum Berlin, Albert-Einstein-Strasse 15, 12489 Berlin, Germany*

(Received 23 December 2008; revised manuscript received 29 June 2009; published 27 August 2009)

Electrons in isolated graphene layers are a two-dimensional gas of massless Dirac Fermions. In realistic devices, however, the electronic properties are modified by elastic deformations, interlayer coupling and substrate interaction. Here, we unravel the electronic structure of noninteracting, doped graphene layers by revisiting the stage one graphite intercalation compound KC_8. To this end we apply angle-resolved photoemission spectroscopy and *ab initio* calculations. The full experimental dispersion is in excellent agreement with calculations of doped graphene once electron correlations are included at the *GW* level (Greens function *G* of the Coulomb interaction *W*). This highlights that KC_8 has negligible interlayer coupling allowing us to access the full experimental Dirac cone.

DOI: 10.1103/PhysRevB.80.075431 PACS number(s): 71.18.+y, 79.60.−i

The recent discovery of two-dimensional metastable graphene sheets has sparked enormous interest in their low-energy electronic structure.[1,2] Angle-resolved photoemission spectroscopy (ARPES) has been proven to be a key tool to determine the electronic structure of one- and few-layer graphene[3] and graphite.[4–6] A major problem for the investigation of graphene on SiC and metal substrates is that there is a significant modification of the electronic structure due to interaction with the substrates yielding charge transfer and hybridization.[7,8] Upon intercalation of Au into the graphene/substrate interface, the Fermi level could be brought back to the Dirac point.[9] However, the graphene electronic bands are still strongly renormalized by a kink at 0.95 eV due to interaction with the Au film.[9] Thus, neither graphene on SiC nor graphene on metal substrates provides access to the full Dirac cone of noninteracting graphene. One way to overcome this problem is to measure single crystalline graphite, which has no substrate interaction. In this case however, a k_z dispersion of two π valence bands[6] and a small gap[10] were observed because of the *AB* stacking of graphene layers (*AA* stacking does not show the gap opening).[11] Another important issue is the renormalization of the bare electronic band structure due to doping-dependent electron-electron correlation,[6] electron-phonon coupling (EPC)[5,12] or electron-plasmon coupling.[13]

In the present work, we take a different perspective to circumvent the problems of substrate interaction, strong bilayer splitting and electron-electron correlation by revisiting stage one graphite intercalation compound (GIC) KC_8 using a combination of ARPES and *ab initio* calculations. We show that the electronic properties of intercalated graphite and graphene are equivalent, therefore, we can use the former to understand the physics of the latter. In particular, we provide the full experimental Dirac cone of doped graphene layers in KC_8 using ARPES. We compare the ARPES intensities to *ab initio* calculations and find good agreement with calculations at the *GW* level. In contrast to previous works on undoped graphite[6] and graphene monolayers on metal substrates[7,14] the electronic energy band structure of graphene sheets in KC_8 is not modified by a k_z dispersion[6] or substrate induced gap opening.[7,14]

GICs have been at the focus of intense research in the last four decades because they have a wide range of tunable electronic properties.[15] In stage I alkali GICs the graphene layers have *AA* stacking and only one π conduction(valence) band and can thus be considered as a doped graphene layer sandwiched in between two positively charged plates. Furthermore, the interlayer distance increases from 3.35 Å to 5.35 Å when going from graphite to KC_8, resulting in a completely flat k_z dispersion (perpendicular to the graphene layers). Thus the low-energy band structure of stage I GICs is identical to doped graphene resulting in a linear π band dispersion close to the crossing point of the valence and conduction bands.[16,17] Experimentally, preliminary studies on ARPES of GICs were reported.[18,19] Until now the details in the low-energy quasiparticle (QP) dispersion of GICs have not been identified and the issue of whether the charge transfer to graphite is complete[20–23] or partial[18,19,24] was never resolved.

Experiments were done at BESSY II using the UE112-PGM2 beamline and a Scienta RS 4000 analyzer yielding a total energy resolution of 15 meV and a momentum resolution better than 0.01 $Å^{-1}$. Natural graphite single crystal samples (~1 cm in diameter) were mounted on a three axis manipulator and cleaved in–situ. Intercalation was performed using commercial getter sources and evaporating potassium onto the graphite crystal for several minutes. Subsequent steps of evaporation with the graphite sample at room temperature

were followed by equilibration for 30 min at 50 C. The distance from the getter source was 7 cm and the total dosing time was 50 min. In order to check the doping level, we measured ARPES after each intercalation step. The proof that we reached stage I was given by the appearance of only one π valence band [instead of 2(3) valence bands for stages II(III)]. In addition stage I compounds are identified by their characteristic golden color. After full intercalation, KC_8 was immediately cooled down by liquid He to 25 K and measured.

The calculations of the electronic dispersion of graphene in a slab geometry (d=20 a.u.) are performed on two levels. First, we calculate the Kohn-Sham band-structure within the LDA to density-functional theory.[25] Wave functions are expanded in plane waves with an energy cutoff at 25 Ha. Core electrons are accounted for by Trouiller-Martins pseudopotentials. In the second step, we use the *GW* approximation[26–28] to calculate the self-energy corrections to the LDA dispersion.[29] For the calculation of the dielectric function $\epsilon(\omega,q)$ we use a Monkhorst-Pack k grid sampling $36\times36\times1$ points and bands up to 70 eV (namely, 50 bands) of the first Brillouin zone (BZ). In addition, we carried out tight-binding (TB) calculations where we have fit the coupling parameters up to third-nearest neighbors (3NN) to the maxima of the ARPES intensity.

The KC_8 crystal structure is given by individual graphene sheets separated by layers of potassium as shown in Fig. 1(a). The fully intercalated graphite crystals have a characteristic golden color as shown in Fig. 1(b). We now carry out a detailed analysis of the QP dispersion of KC_8 as measured by ARPES. In Fig. 1(c) the absence of photoemission intensity at the BZ center (Γ point) is put into evidence. This experimental result is in good agreement to *GW* calculations which predict a potassium 4s derived band at the Γ point *above* E_F. We also performed measurements with different photon energies in order to exclude effects due to optical matrix elements. Interestingly, calculations on the local-density approximation (LDA) level predict this band *below* E_F. In Fig. 1(d), we show energy dispersion curves (EDC) and cuts of the π bands that intersect the corners of the BZ. We also measured the photon energy dependence and we do not observe a dispersion perpendicular to the layers, in stark contrast to undoped graphite.[6] Figure 1(e) shows the equienergy cuts of the raw photoemission intensity. Note that here the K point is at k_x=k_y=0 and that the k_x axis corresponds to the KM direction. When moving from the cut at E_F to lower energies the circumference of the equienergy contour of the conduction band becomes smaller. Evidently we have one π valence and one π conduction band and they meet in one point. Therefore, in analogy to graphene, the crossing point at 1.35 eV is from now on called the "Dirac point." Decreasing the energy of the cut below 1.35 eV enlarges the equienergy contour of the valence band. Comparing two contours with the same distance from the Dirac point [e.g., cuts at E_F and 2.7 eV in Fig. 1(e)], it can be seen that the π valence band is steeper and has less trigonal warping. Such a result is related to the fact that the self-energy corrections to the trigonal warping effect increase with doping.[30] Interestingly, as depicted in Fig. 1(e), the photoemission matrix elements of the valence and conduction bands are complementary yielding a high-photoemission intensity in 1/3 and 2/3 of the BZ, respectively (the asymmetry in the photoemission intensity is attributed to the dipole matrix element similarly to the case of pristine graphite in Ref. 6). From the contour at E_F in Fig. 1(e), we determine the number of carriers n_e by integrating the volume inside the Fermi surface. This yields a charge transfer of ~0.8 electrons/potassium atom, close to a complete charge transfer. From these results, concomitant with the absence of any Fermi surface of K 4s states close to the Γ point [see Fig. 1(c)] we can safely conclude an almost complete charge transfer from potassium in agreement with previous results.[20–23]

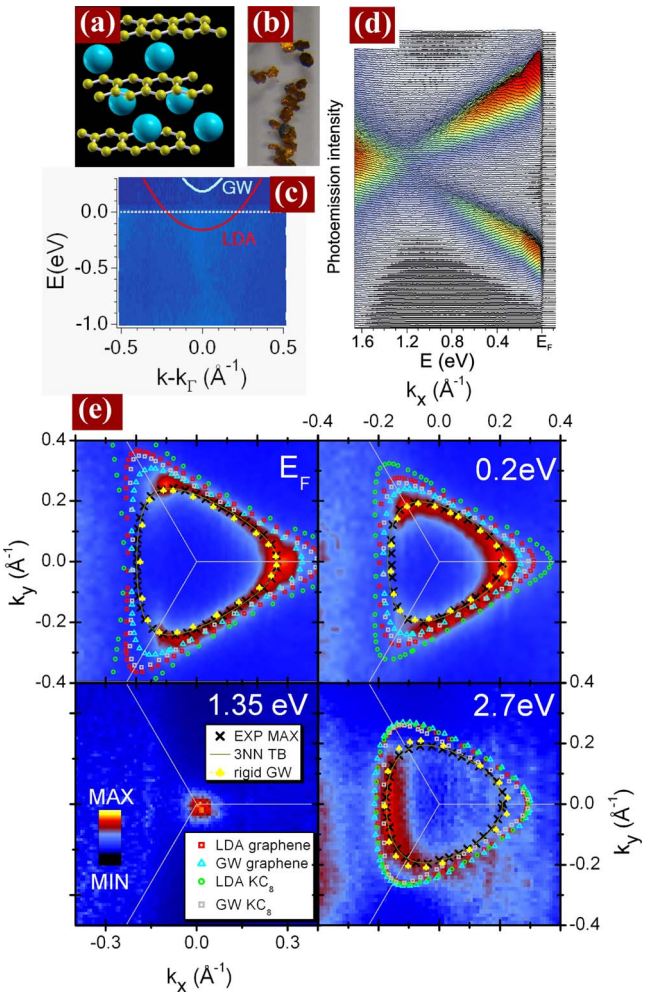

FIG. 1. (Color online) (a) Crystal structure of KC_8. (b) Photo of intercalated KC_8 single crystals with golden color. (c) Region close Fermi level measured from the Γ point of the BZ to put in evidence the lack of photoemission signal. Lines denote LDA and *GW* calculations. (d) As measured EDC cuts through the corner of the 3D BZ. (e) Equienergy contours of the photoemission intensity taken at 48 eV photon energy for four binding energies along with calculations at the LDA and *GW* level and a 3NN TB fit (see text).

A deeper understanding of the underlying band structure is gained by comparing (un)doped graphene and KC_8, experiments and first-principle calculations at different levels of the theory [from the widely used TB and LDA with the one shot and partial-self-consistent *GW* (Refs. 26–28)], which are also shown in Fig. 1(e). Concerning the *ab initio*

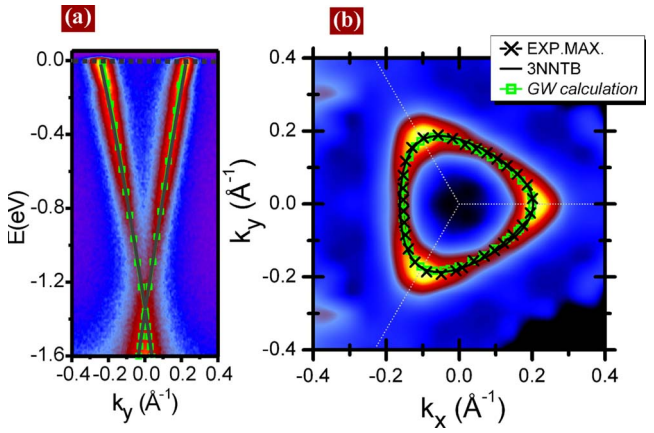

FIG. 2. (Color online) (a) ARPES scan measured close to the k_y direction along with the TB fit of the bare-band dispersion (black) and the *GW* calculation for rigidly doped graphene (green). (b) Symmetrized equienergy contour for $E=0.24$ eV and maxima (crosses) along with the TB fit and the *GW ab initio* calculations.

calculations, we found that the *GW* approximation yields the best agreement to the experimental results of KC_8. We have calculated both, undoped graphene with a rigid band shift and doped graphene. It is found that the *GW* calculations for graphene and application of a rigid band shift of 1.35 eV yield perfect agreement to the experiment. It can clearly be seen from Fig. 1(e) that the LDA calculations for both, graphene and KC_8 underestimate the steepness of the bands and are in unsatisfactory agreement with the ARPES. We also found that the QP dispersion at K concomitant with the lack of photoemission intensity at the Γ point in KC_8 is very well reproduced by calculations on the *GW* level. The results for a cut through K point are depicted in Fig. 2. Both, the observed linear dispersion, which is reminiscent of the underlying structure of the graphene parent compound and the equienergy contour of the photoemission intensity at E_F are in perfect agreement to the *GW* calculations of graphene. This clearly indicates that electron-electron correlation is crucial to explain the size of the Fermi surface and the observed trigonal warping. I.e., similar to graphite,[6] electron-electron correlation is at the heart of the band structure of the underlying (doped) graphene layers. This is in stark contrast to calculations on the LDA level which have too small band velocities and are yielding an incomplete charge transfer together with a partially occupied K 4*s* band in the vicinity of the Γ point. Hence, our results unambiguously highlight the following facts inherent to the electronic structure of doped graphene without substrate interaction: (i) the dispersion the Dirac Fermions depends on the doping level and the equienergy contours above and below the Dirac point are anisotropic; (ii) the trigonal warping increases with increasing doping level; (iii) in KC_8 each potassium atom transfers nearly one electron to the graphene layers.

As can be seen in Figs. 1 and 2 the ARPES intensity maxima at E_F and the linear dispersion close to the Dirac point are very well described by both, the *GW* calculation for graphene with a rigid band shift and a TB calculation. In order to quantitatively reproduce the shape of the contours we had to include up to three nearest neighbors in the TB

TABLE I. Parameters of the 3NN TB fit to the ARPES experiment. $\gamma_0-\gamma_2$ and s_1-s_2 are the transfer and overlap integrals, respectively. The on-site energy is given by ε_{2p}. These parameters were used to calculate the 3NN TB band structures from Figs. 1 and 2. All values except the ones for s_0-s_2 are in eV.

γ_0	γ_1	γ_2	s_0	s_1	s_2	ε_{2p}
−2.937	−0.286	−0.265	0.025	0.068	0.059	1.937

calculations, similar to the case of graphite and few layer graphene.[11] All previous TB descriptions of KC_8 did not consider these higher order interactions. However, they are needed because we cannot reproduce the strong trigonal warping of the experimental equienergy contours in Fig. 1 by the nearest neighbor TB calculation. Note that the structure of the 3NN TB Hamiltonian for KC_8 is the same as for the case of pristine graphene and given in Ref. 11. For future works, we list in Table I the 3NN TB parameters that can be used to reproduce the experimental electron energy band structure. These parameters are fit to the experimental ARPES maxima excluding a small region below E_F, which is modified by the electron-phonon interaction.[31] Since the measured region is limited to a part of the π valence band (shown in Figs. 1 and 2), this set of TB parameters is slightly different to the one fit to *GW* calculations, which includes the full π and π^* bands[31] although the resulting bands are in very good agreement. The electron-phonon interaction results in a kink in the quasiparticle dispersion at 166 meV and we employed the present TB calculation as the bare band structure for a self-consistent analysis of the complex self-energy function.[31] By an accurate comparison to the phonon dispersion relation we can unambiguously assign this kink to the coupling to an in-plane TO phonon from the K point of the Brillouin zone,[31,32] similar to the case of graphene on SiC.[33] The relevant photohole relaxation process is scattering between K and K' points of the BZ.

Let us now turn to one of the main results of the present work, unravelling the full experimental Dirac cone. For this purpose we extracted the photoemission maxima for binding energies between E_F and 3 eV in steps of 10 meV. The results are depicted in Fig. 3(a). It is obvious that the two-dimensional band structure close to the Dirac point is linear and two bands meet each other in one point. This argument puts in evidence that in KC_8 far from the Fermi level but close to the Dirac point the dispersion of the electronic bands is not different for graphene. This highlights that KC_8 indeed consists of noninteracting doped sheets of graphene, in contrast to previous experiments on substrate based graphene where there is a gap opening,[7,34] although the origin of this gap is still heavily debated.[35] This gap causes a breakdown of massless Dirac Fermions which has profound limitation on the observation of relativistic physics in graphene as it causes the π electrons to acquire a small but finite rest mass as outlined in.[11] Therefore the spectroscopic investigation of doped graphene layers in KC_8 provides an elegant solution to this problem.

From the previous discussion the analysis of the full two-dimensional dispersion of KC_8 around the Dirac point can

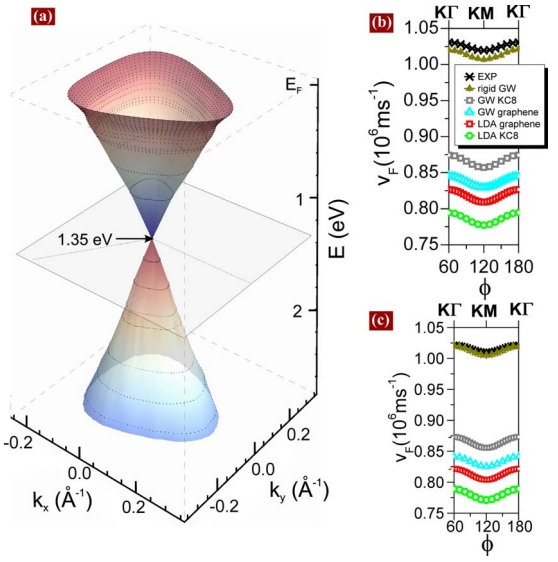

FIG. 3. (Color online) (a) Experimental Dirac cone from the observed photoemission intensity maxima (denoted as dots). Measured and calculated (*GW*) values of v_F for (b) electrons and (c) holes around the Dirac point.

thus actually be used to learn about the physics of graphene. To further support the validity of this analogy we analyze the experimental direction dependent v_F in the region of 0.05 eV above and below the Dirac point. These results for the valence and conduction band along with the LDA and *GW* calculations of doped graphene are depicted in Figs. 3(b) and 3(c), respectively. The v_F are very anisotropic and have a maximum (minimum) in $K\Gamma(KM)$ direction. This anisotropy is already captured by the LDA for both, KC_8 and doped graphene. However, the absolute values are underestimated in the case of LDA. In order to obtain better agreement between experiment and theory one needs to go to *GW* calculations, which capture the electron-electron correlation. If we take the *GW* for graphene and apply a rigid band shift model, the agreement is perfect as can be seen from Fig. 3. This holds for both the valence and the conduction band v_F, which have almost the same absolute value. The very good quantitative agreement highlights the validity of our approach. In close similarity to our results on pristine graphite,[6] we observed that electron-electron correlation is crucial to explain the band structure of doped graphene layers in KC_8.

In conclusion, we have synthesized KC_8 *in situ* and performed high-resolution ARPES measurements. We found an almost complete charge transfer of potassium to graphene and the complete absence of interlayer interaction. Therefore by measuring the conical band dispersion of KC_8 we have access to the valence and conduction Dirac Fermions of graphene. Our results circumvent the problems which are associated with strong substrate interaction of graphene[7,34,35] or with interlayer interaction,[6] both of which cause a breakdown of Dirac Fermions picture. Most importantly, we unraveled the full experimental Dirac cone of graphene and evaluated the anisotropy of the momentum dependent v_F in the valence and conduction band. Those findings provide crucial input for the understanding of the unique electronic and transport properties of graphene. The measured and the calculated QP band structure of KC_8 follows the one for graphene after including self-energy corrections at the *GW* level that describe the increase the slope of the bands due to electron-electron correlation effects when compared to the LDA calculations. In addition we showed that a 3NN TB method reproduces the measured equienergy contours.

A.G. acknowledges an APART fellowship from the Austrian Academy of Sciences and a Marie Curie Reintegration grant from the EU ("ECO-GRAPHENE"). T.P. acknowledges DFG for Project No. PI 440/3/4/5. D.V. acknowledges DFG for Grant No. VY 64/1-1. C.A. and A.R. acknowledge funding by the Spanish MEC (Grant No. FIS2007-65702-C02-01), "Grupos Consolidados UPV/EHU del Gobierno Vasco" (Grant No. IT-319-07), and the European Community through NoE Nanoquanta (Grant No. NMP4-CT-2004-500198), e-I3 ETSF project (INFRA-2007-1.2.2: Grant No. 211956), and SANES (Grant No. NMP4-CT-2006-017310). The computer resources were provided by the Barcelona Supercomputing Center and the Basque Country University UPV/EHU (SGIker Arina) and ETSF. J.F. acknowledges financial support from the DFG (Forschergruppe No. FOR 538).

*Corresponding author; ag3@biela.ifw-dresden.de

[1] A. Geim and K. Novoselov, Nature Mater. **6**, 183 (2007).
[2] K. S. Novoselov, A. K. Geim, S. V. Morozov, D. Jiang, Y. Zhang, S. V. Dubonos, I. V. Grigorieva, and A. A. Firsov, Science **306**, 666 (2004).
[3] T. Ohta, A. Bostwick, T. Seyller, K. Horn, and E. Rotenberg, Science **313**, 951 (2006).
[4] S. Y. Zhou, G.-H. Gweon, J. Graf, A. V. Fedorov, C. D. Spataru, R. D. Diehl, Y. Kopelevich, D.-H. Lee, S. G. Louie, and A. Lanzara, Nat. Phys. **2**, 595 (2006).
[5] K. Sugawara, T. Sato, S. Souma, T. Takahashi, and H. Suematsu, Phys. Rev. Lett. **98**, 036801 (2007).
[6] A. Grüneis, C. Attaccalite, T. Pichler, V. Zabolotnyy, H. Shiozawa, S. L. Molodtsov, D. Inosov, A. Koitzsch, M. Knupfer, J. Schiessling, R. Follath, R. Weber, P. Rudolf, L. Wirtz, and A. Rubio, Phys. Rev. Lett. **100**, 037601 (2008).
[7] A. Grüneis and D. V. Vyalikh, Phys. Rev. B **77**, 193401 (2008).
[8] S. Kim, J. Ihm, H. J. Choi, and Y.-W. Son, Phys. Rev. Lett. **100**, 176802 (2008).
[9] A. Varykhalov, J. Sanchez-Barriga, A. M. Shikin, C. Biswas, E. Vescovo, A. Rybkin, D. Marchenko, and O. Rader, Phys. Rev. Lett. **101**, 157601 (2008).
[10] M. Orlita, C. Faugeras, G. Martinez, D. K. Maude, M. L. Sadowski, and M. Potemski, Phys. Rev. Lett. **100**, 136403 (2008).
[11] A. Grüneis, C. Attaccalite, L. Wirtz, H. Shiozawa, R. Saito, T. Pichler, and A. Rubio, Phys. Rev. B **78**, 205425 (2008).
[12] J. L. McChesney, A Bostwick, T Ohta, K. V. Emtsev, T Seyller, K. Horn, and E Rotenberg, arXiv:0705.3264 (unpublished).

[13] A. Bostwick, T. Ohta, T. Seyller, K. Horn, and E. Rotenberg, Nat. Phys. **3**, 36 (2007).
[14] A. Grüneis, K. Kummer, and D. V. Vyalikh, New J. Phys. **11**, 073050 (2009).
[15] M. S. Dresselhaus and G. Dresselhaus, Adv. Phys. **30**, 139 (1981).
[16] J. Blinkowski, N. H. Hau, C. Rigaux, J. P. Vieren, R. L. Toullec, G. Furdin, A. Herold, and J. Melin, J. Phys. (France) Lett. **41**, 47 (1980).
[17] R. Saito and H. Kamimura, Phys. Rev. B **33**, 7218 (1986).
[18] W. Eberhardt, I. T. McGovern, E. W. Plummer, and J. E. Fischer, Phys. Rev. Lett. **44**, 200 (1980).
[19] N. Gunasekara and T. Takahashi, Z. Phys. B: Condens. Matter **70**, 349 (1988).
[20] G. Wang, W. R. Datars, and P. K. Ummat, Phys. Rev. B **44**, 10880 (1991).
[21] M. T. Johnson, H. I. Starnberg, and H. P. Hughes, Solid State Commun. **57**, 545 (1986).
[22] J. Algdal, T. Balasubramamian, M. Breitholtz, T. Kihlgren, and L. Wallden, Surf. Sci. **601**, 1167 (2007).
[23] J. M. Zhang and J. Eklund, Mater. Res. **2**, 858 (1987).
[24] P. Oelhafen, P. Pfluger, E. Hauser, and H. J. Güntherodt, Phys. Rev. Lett. **44**, 197 (1980).
[25] X. Gonze, J. M. Beuken, R. Caracas, F. Detraux, M. Fuchs, G. M. Rignanese, L. Sindic, M. Verstraete, G. Zerah, F. Jollet, M. Torrent, A. Roy, M. Mikami, Ph. Ghosez, J. Y. Raty, and D. C. Allan, Comput. Mater. Sci. **25**, 478 (2002).
[26] M. S. Hybertsen and S. G. Louie, Phys. Rev. B **34**, 5390 (1986).
[27] L. Hedin, Phys. Rev. **139**, A796 (1965).
[28] S. G. Louie, in *Topics in Computational Materials Science*, edited by C. Y. Fong (World Scientific, Singapore, 1997), p. 96.
[29] A. Marini *et al.*, the Yambo project, http://www.yambo-code.org/.
[30] R. Roldan, M. P. Lopez-Sancho, and F. Guinea, Phys. Rev. B **77**, 115410 (2008).
[31] A. Grüneis, C. Attaccalite, A. Rubio, D. V. Vyalikh, S. L. Molodtsov, J. Fink, R. Follath, W. Eberhardt, B. Büchner, and T. Pichler, Phys. Rev. B **79**, 205106 (2009).
[32] A. Grüneis, J. Serrano, A. Bosak, M. Lazzeri, S. L. Molodtsov, L. Wirtz, C. Attaccalite, M. Krisch, A. Rubio, F. Mauri, and T. Pichler, Phys. Rev. B **80**, 085423 (2009).
[33] S. Y. Zhou, D. A. Siegel, A. V. Fedorov, and A. Lanzara, Phys. Rev. B **78**, 193404 (2008).
[34] S. Y. Zhou, G. H. Gweon, A. V. Fedorov, P. N. First, W. A. de Heer, D. H. Lee, F. Guinea, A. H. Castro Neto, and A. Lanzara, Nature Mater. **6**, 916 (2007).
[35] S. Y. Zhou, D. A. Siegel, A. V. Fedorov, F. El Gabaly, A. K. Schmid, A. H. Castro Neto, D.-H. Lee, and A. Lanzara, Nature Mater. **7**, 259 (2008).